RECENT SHELL-MODEL CALCULATIONS OF γ-DECAY STRENGTH FUNCTIONS*

Kamila Sieja

Université de Strasbourg, IPHC, 23 rue du Loess, 67037 Strasbourg, France
and
CNRS, UMR7178, 67037 Strasbourg, France

Stephane Goriely†

Institut d'Astronomie et d'Astrophysique, Université Libre de Bruxelles
CP-226, 1050 Brussels, Belgium

(Received January 29, 2020)

We present recent shell-model calculations of the γ-decay in sd–pf- and pf-shell nuclei. We focus on the M1 part of the dipole strength which was shown to exhibit interesting low-energy effects, in particular a low-energy enhancement which can have a considerable impact on the radiative neutron capture. We discuss the persistence of the shell effects in the nuclear quasi-continuum and the relation between the shape of the strength function at low-energy and nuclear deformation.

DOI:10.5506/APhysPolBSupp.13.535

1. Introduction

Theoretical calculations of the neutron capture cross sections within the Hauser–Feshbach model [1] require the knowledge of the γ-decay probability of the compound nucleus which is characterized by a statistical de-excitation strength function. It is known that the photon strength function is dominated by the dipole component which has traditionally been modeled by simple Lorentzian approximations with some energy dependence [2]. Such models, however, cannot describe structure effects at lowest γ energies which were shown to have a considerable impact on the calculated neutron capture

* Presented at the XXVI Nuclear Physics Workshop *Key problems of nuclear physics*, Kazimierz Dolny, Poland, September 24–29, 2019.

† An F.R.S.-FNRS research associate.

cross sections for exotic neutron-rich nuclei [3]. A systematic microscopic evaluation of dipole strength functions was achieved in the QRPA approach [4, 5], however only for the photoabsorption strength. In recent years, dipole strength functions have also been obtained within the large-scale shell model (SM) in several regions of the nuclear chart [6–12], proving the capacity of this framework to provide at least qualitative explanation of low-energy effects revealed by experimental data. In particular, in Ref. [11], a first microscopic calculation of both dipole modes was performed, showing a different behavior of the E1 and M1 strengths at low transition energy. The trends predicted by shell model were later incorporated to a semi-empirical, global description of γ-decay strengths for applications in Ref. [13], showing an overall improvement of the calculated radiative widths and neutron capture cross sections as compared to those obtained using simple analytical prescriptions for the de-excitation strength functions. It was also predicted that such an upbend of the M1 strength towards $E_\gamma = 0$, if present, can considerably affect the calculated neutron capture rates.

Shell-model studies suggested, however, that the enhancement of the low-energy M1 strength is most probable near closed shells, where protons and neutrons occupy high-j orbitals of different parity and that the low-energy strength can be shifted to the scissors mode in deformed nuclei [7]. A relation between the strength at low energy and B(E2) values, being the measure of nuclear deformation, was also presented in Ref. [12]. In the present work, we explore further shell-model systematic calculations in pf and sd–pf nuclei, which shed more light on the relation between the low-energy behavior of the M1 strength and the nuclear shape.

2. De-excitation strength function in the shell-model framework

In the following, we present systematic calculations of the de-excitation M1 strength function in a number of isotopic chains that can be described in the sd–pf and pf model spaces. In the present calculations, we treat the full model space and use well-established shell-model interactions SDPF-U [14] and LNPS [15], respectively. A standard quenching factor of 0.75 is applied to the spin part of the magnetic dipole operator. The de-excitation strength function is obtained from the Bartholomew definition [16]

$$f_{\mathrm{M1}}\left(E_\gamma, E_\mathrm{i}, J_i, \pi\right) = 16\pi/(9\hbar c)^3 \langle B(\mathrm{M1})\rangle \rho\left(E_i, J_i, \pi\right) , \qquad (1)$$

where $\rho_i(E_\mathrm{i}, J_i, \pi)$ is the partial level density determined at a given initial excitation energy E_i and $\langle B(\mathrm{M1})\rangle$ the average decay probability for an energy interval. For each nucleus, we calculate 60 excited states in the spin range of $J = 0$–7 for even and odd–odd nuclei, and $J = 1/2$–$15/2$ for the odd ones. This typically leads to $\sim 2 \times 10^4$ of M1 matrix elements used in

the averaging of $\langle B(\mathrm{M1})\rangle$ values in Eq. (1). Such a treatment was shown to provide strength functions which can be directly compared to experiment and give a qualitative explanation of the latter [6–12].

In Fig. 1, we show the results of shell-model calculations in the even–even isotopes of sulfur, argon and calcium as well as in the odd–even chlorine nuclei. As seen, the magnitude of the f_{M1} is rather independent of the mass number for the lowest γ energies. Slightly different trends can be observed between isotopic chains and between isotopes in a given chain, as will be made more explicit in the next section.

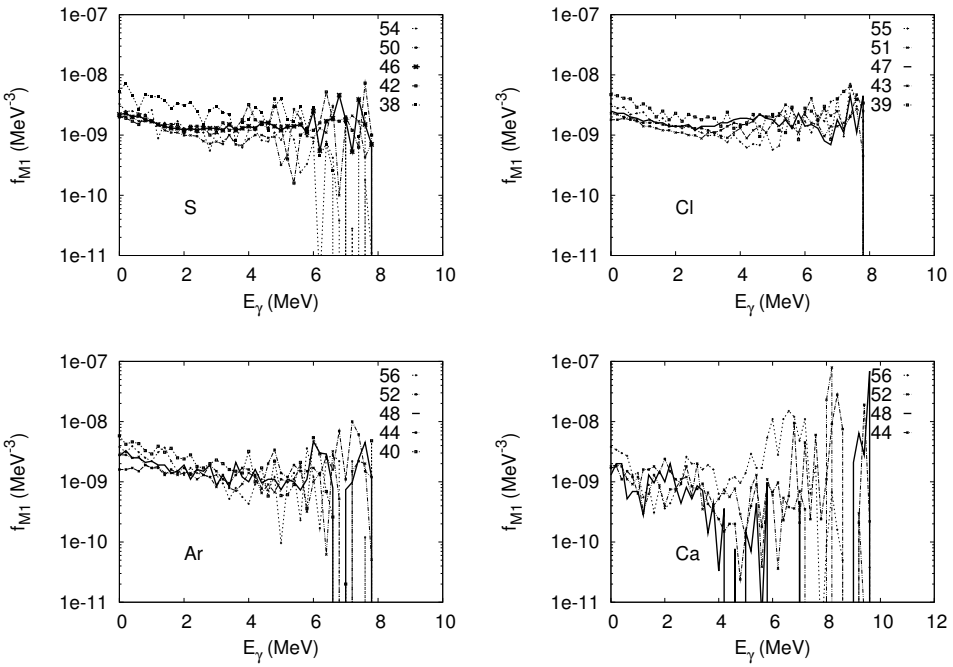


Fig. 1. De-excitation M1 strength functions obtained by shell-model calculations in several isotopic chains.

We also present, in Fig. 2, a systematic M1 calculation of selected pf-shell nuclei, namely titaniums and chromiums. These two chains exhibit a different behavior: while nearly all the titanium isotopes have an upbend in their strength function, no such upbend is present in the chromiums, up to ^{51}Cr. One should stress that ^{48}Cr is a model example of a prolate-deformed rotor in the pf-shell and its closest neighbours are also well deformed. As was stressed before, such deformed systems do not posses a spike at the lowest transition energy but a rather flat form of the f_{M1} towards $E_\gamma = 0$.

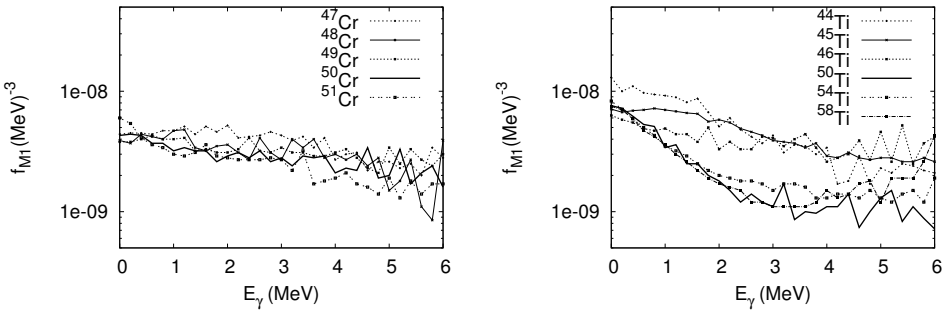


Fig. 2. De-excitation M1 strength functions obtained by shell-model calculations in Cr and Ti chains.

3. Shell effects in the nuclear quasi-continuum

The trends observed in the γ-ray strength function plotted in Figs. 1 and 2 are entirely due to the behavior of the averaged B(M1) strength in the considered nuclei (meaning the shape of f_{M1} is independent of the calculated level density). As we stated above, the appearance of the upbend is related to the proximity of shell closures and occupancies of specific neutron and proton orbitals. In particular, the authors of Ref. [10] plotted a ratio of averaged B(M1) values in the energy intervals 0–2 MeV and 2–6 MeV, *i.e.* $\frac{\langle B(\mathrm{M1})\rangle(0-2\,\mathrm{MeV})}{\langle B(\mathrm{M1})\rangle(2-6\,\mathrm{MeV})}$. Such a representation showed a clear correlation between the upbend and the proximity of a shell closure, *i.e.* the ratio in *sd* and *pfg* nuclei, with a few exceptions, exhibited a parabolic trend typical of the 2^+ excitation energies along the isotopic chains.

In the following, we extract the ratio of the averaged B(M1) strength in the calculated isotopic chains from the *sd*–*pf* shell, where the $N = 20, 28$ and $N = 40$ shell closures should influence the behavior of the low-energy strength, see Fig. 3.

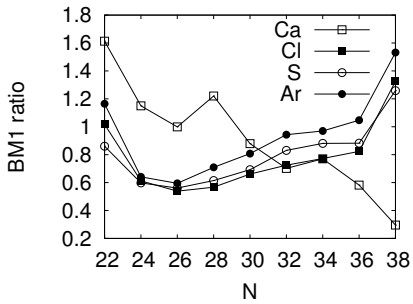


Fig. 3. Ratio of the averaged B(M1) strengths in calculated nuclei. See the text for details.

As can be noted, the ratio peaks towards the $N = 20$ closure for all the isotopic chains. The $N = 40$ sub-closure is predicted to exist in the S, Ar and Cl isotopes but disappears for the calcium chain. ^{60}Ca was studied in Ref. [15] and suggested to have a considerable $4p$–$4h$ component in its ground state in accordance with the present observation of no-shell effect in the f_{M1}. In contrast, the $N = 28$ shell closure is visible only in calcium. This is consistent with the current evidence for the sulfur isotopes, where the shape-coexistence was found at $N = 28$ [17, 18]. On the contrary, the $N = 28$ closure in ^{46}Ar was predicted from mass measurements, 2^+ energies and from B(E2) values, see *e.g.* [19, 20]. Interestingly, the present interaction reproduces well the first two but not the E2 transition strength. It was shown in Ref. [20] that none of the available shell-model interactions in the *sd*–*pf* model space is able to reproduce the experimental value of $B(\mathrm{E2}; 2^+ \rightarrow 0^+)$ in ^{46}Ar. One can thus expect that a similar problem concerns the magnetic transition strengths and that the de-excitation strength function may be influenced by the $N = 28$ shell closure also in the argon chain.

The independence of the γ-ray strength function of excitation energy, which was tested in the present and in many other shell-model calculations, means that the shell effects are also independent of the excitation energy and survive close to the neutron threshold. Thus, the γ-ray de-excitation strength function can be used as another probe of the shell effects and of their persistency at higher excitation energies.

4. Deformation dependence of the low-energy M1 limit

In our previous work [13], we introduced an empirical low-energy contribution to the M1 and E1 de-excitation strength function to complement the axially-symmetric QRPA predictions based on HFB calculations with the Gogny D1M interaction [4, 5]. In particular, the so-called D1M+QRPA+0lim de-excitation M1 strength function was expressed as

$$\overleftarrow{f_{\mathrm{M1}}}(E_\gamma) = f_{\mathrm{M1}}^{\mathrm{QRPA}}(E_\gamma) + C\ \mathrm{e}^{-\eta E_\gamma}\,, \tag{2}$$

where $f_{\mathrm{M1}}^{\mathrm{QRPA}}$ is the D1M+QRPA M1 strength function at the photon energy E_γ and $C \simeq 10^{-8}$ MeV^{-3}, $\eta = 0.8$ MeV^{-1} are free parameters that were adjusted on shell-model results and available low-energy experimental data such as those obtained with the Oslo method [21–23]. However, due to the lack of systematic calculations, the low-energy limit of the M1 strength was assumed to be deformation-independent. A first attempt to determine the deformation dependence of this M1 low-energy enhancement was done in Ref. [24] on the basis of experimental data where constraints could be imposed from multistep γ-cascade spectra extracted from neutron capture on isolated resonances. The resulting experimentally constrained C values

are shown in Fig. 4. Such a multistep cascade data is available for a set of 15 nuclei only, mainly deformed, including isotopes of Mo, Cd, Gd, Dy and U. For this reason, it was proposed to adopt a lower limit, $C = 10^{-8}$ MeV^{-3}, for all nuclei with $A \gtrsim 105$ and for lighter nuclei, a simple deformation-dependent $C = 3 \times 10^{-8} \exp(-4\beta_{20})$ MeV^{-3} [24, 25]. The corresponding prescription is shown in Fig. 4 (right panel). With the present large-scale SM calculations, as presented in Sect. 2, it is possible to test the relevance of such a prescription.

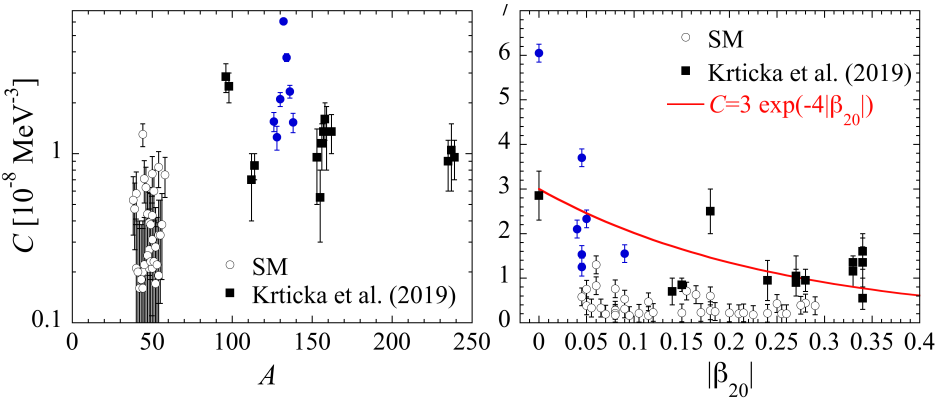


Fig. 4. SM (circles) and experimental (squares) [24] estimates of the low-energy enhancement factor C as a function of the atomic mass A (left panel) of D1M deformation parameter β_{20}. The open black circles correspond to SM calculations presented in Sect. 2 and the solid circles to SM calculations for nuclei in the vicinity of ^{138}Ba [12]. The curve is the simple empirical energy-dependence adopted in Ref. [25]. An error bar of 0.2×10^{-8} MeV^{-3} has been included in all SM estimates.

The SM and experimentally constrained [24] estimates of the low-energy enhancement factor C are summarized in Fig. 4 as a function of the atomic mass A and of the deformation quadrupole parameter β_{20}. C values lower than 10^{-8} MeV^{-3} are obtained for light sd and pf nuclei. While non-negligible quadrupole deformation may be derived by mean-field models (see Fig. 4, right panel), those nuclei are known as being vibrational, so that the D1M determination of their static deformation may not be the right description. In this case, the exponentially decreasing prescription as a function of the deformation, as proposed in Ref. [24, 25], is clearly not satisfactory. Significantly larger C values between 1 and 6×10^{-8} MeV^{-3} are predicted by the SM for the spherical $N \simeq 82$ nuclei reaching this maximum value for ^{132}Te [12]. A rather similar value was extracted from multistep γ-cascade spectra for the ^{96,98}Mo isotopes.

The present comparison clearly shows that the simple prescription used so far, both as a function of A and β_{20}, may not be adequate to describe the complex structure of this low-energy contribution to the M1 de-excitation strength function and that much more theoretical and experimental work is needed.

REFERENCES

[1] H. Feshbach, C. Porter, V. Weiskopf, *Phys. Rev. C* **96**, 448 (1954).
[2] R. Capote *et al.*, *Nucl. Data Sheets* **110**, 3107 (2009).
[3] A.C. Larsen, S. Goriely, *Phys. Rev. C* **82**, 014318 (2010).
[4] M. Martini *et al.*, *Phys. Rev. C* **94**, 014304 (2016).
[5] S. Goriely *et al.*, *Phys. Rev. C* **94**, 044306 (2016).
[6] R. Schwengner, S. Frauendorf, A.C. Larsen, *Phys. Rev. Lett.* **111**, 232504 (2013).
[7] R. Schwengner, S. Frauendorf, B.A. Brown, *Phys. Rev. Lett.* **118**, 092502 (2017).
[8] B.A. Brown, A.C. Larsen, *Phys. Rev. Lett.* **113**, 252502 (2014).
[9] A.C. Larsen *et al.*, *Phys. Rev. C* **97**, 054329 (2018).
[10] J.E. Midtbø *et al.*, *Phys. Rev. C* **98**, 064321 (2018).
[11] K. Sieja, *Phys. Rev. Lett.* **119**, 052502 (2017).
[12] K. Sieja, *Phys. Rev. C* **98**, 064312 (2018).
[13] S. Goriely, S. Hilaire, S. Péru, K. Sieja, *Phys. Rev. C* **98**, 014327 (2018).
[14] F. Nowacki, A. Poves, *Phys. Rev. C* **79**, 014310 (2009).
[15] S.M. Lenzi, F. Nowacki, A. Poves, K. Sieja, *Phys. Rev. C* **82**, 054301 (2010).
[16] G. Bartholomew *et al.*, *Adv. Nucl. Phys.* **7**, 229 (1972).
[17] C. Force *et al.*, *Phys. Rev. Lett.* **105**, 102501 (2010).
[18] J.L. Egido, M. Borrajo, T.R. Rodríguez, *Phys. Rev. Lett.* **116**, 052502 (2016).
[19] «Atomic mass evaluation 2016», `http://amdc.impcas.ac.cn/`
[20] S. Calinescu *et al.*, *Phys. Rev. C* **93**, 044333 (2016).
[21] A. Voinov *et al.*, *Phys. Rev. Lett.* **93**, 142504 (2004).
[22] M. Guttormsen *et al.*, *Phys. Rev. C* **71**, 044307 (2005).
[23] E. Algin, U. Agvaanluvsan *et al.*, *Phys. Rev. C* **78**, 054321 (2008).
[24] M. Krticka *et al.*, *Phys. Rev. C* **99**, 044308 (2019).
[25] S. Goriely *et al.*, *Eur. Phys. J. A* **55**, 172 (2019).